Earth Science Informatics
https://doi.org/10.1007/s12145-023-00974-0

METHODOLOGY

Determining the time response in GNSS tomographic modeling of troposphere

Elaheh Sadeghi[1] · Masoud Mashhadi Hossainali[2] · Abdolreza Safari[1]

Received: 21 November 2022 / Accepted: 18 February 2023

Abstract

GNSS tomography is a method for the three-dimensional reconstruction of wet refractivity (N_w) in a set of voxels, each covering a specific part of the troposphere. The substantial assumption is the homogeneity of atmosphere in each voxel in given time intervals, known as the time response of model. Determining the optimal time resolution is one of the existing challenges in the tomography of the Earth's atmosphere. We apply Empirical Orthogonal Functions (EOFs) to find an optimal time response for our tomographic model. To investigate our method, we compute the EOFs using the numerical atmospheric model that is available in our test area as the reference field on an already designed tomographic model. Using time resolutions of 30, 45, 60, 75, 90, 105 and 120 min, our EOF based method suggests the time periods of 60 to 75 and 75 to 90 min as the time response in the two days (a dry and a wet day) of our experiments, respectively According to our analysis, because of the quality of our reference field, it is not possible to expect similarities better than 85% for wet day and 93% for dry days in the scattering of the N_w field between the reconstructed images and our reference model.

Keywords GPS tomography · Wet refractivity · Time resolution · Time response · Atmospheric dynamics · EOF

Introduction

Water vapor has an obvious role in the hydrological cycle and plays a key role in energy transport. Therefore, monitoring and determining its changes and distribution is demanding. However, the low spatiotemporal resolution of water vapor sensors and their high cost make it difficult. Bevis et al. (1992) explained how to derive Integrated Water Vapor (IWV) from the Slant Tropospheric Delays (STD) of the GPS signals. Then, Flores et al. (2000) developed a four-dimensional water vapor map by ground-based GNSS networks using voxel-based tomography method.

In voxel-based tomography, troposphere is divided into several cubes known as voxels (Flores et al. 2000) and the wet refractivity (N_w) or water vapor content is computed in each voxel over time intervals known as the time resolution or time response of the tomographic model. N_w or water vapor content as unknown parameters are assumed homogenous and constant in every voxel during the period of reconstructing a tomographic image. GNSS signals pass through many of the voxels while some voxels may remain empty. As the result, GPS-tomography is a mixed determined inverse problem. This makes the application of additional constraints and the regularization techniques inevitable (Rohm and Bosy 2009; Bender et al. 2011; Trzcina and Rohm 2019). Various methods have been proposed for finding a unique solution when reconstructing a tomographic image (Flores et al. 2000; Bender et al. 2009; Heublein et al. 2019).

In addition to the size of voxels, the time response of a model has an evident role in the uniqueness of the tomographic solution: Decreasing the time response reduces the redundancy of the problem and increases the number of empty voxels. In this regard, proposed approaches try to minimize the impact of the time resolution on reconstructed tomographic images: Yao and Zhao (2016) eliminated the

Communicated by: H. Babaie

✉ Elaheh Sadeghi
Sadeghi.Elaheh@ut.ac.ir

[1] School of Surveying and Geospatial Engineering, College of Engineering, University of Tehran, North Kargar Street, Central Building of the College of Engineering, Tehran 1439957131, Iran

[2] Faculty of Geodesy and Geomatics Engineering, K. N. Toosi University of Technology, No. 1346, ValiAsr Street, Mirdamad Cross, Tehran, Iran

Published online: 03 March 2023

empty voxels from the tomographic model. Adavi and Mashhadi-Hossainali (2014) used the concept of Virtual Reference Station (VRS) to fix the rank deficiency of the problem. Some researchers focused on the multi-GNSS tomography, i.e. the combination of the GPS, GLONASS and Galileo systems in reconstructing the tomographic images (Bender et al. 2011, Dong and Jin 2018, Adavi et al. 2022). Some studies also report on the application of the function based approach in troposphere tomography (Haji-Aghajany et al. 2020a, b).

Reconstructed tomographic images not only should lay out the spatial variations of desired parameter (e.g. water vapor) but also, they should include information on the temporal variation of the sought parameter. So far, the proposed methods systematically ignore the dynamics of the Earth's atmosphere. Normally, the time resolution for reconstructed tomographic images is fixed, one hour for example. Therefore, water vapor is assumed to change in each voxel hourly (Bender et al. 2013; Wang and Dessler 2020). Depending on the atmospheric conditions, the time variation of water vapor may happen in shorter or longer periods of time. Moreover, water vapor may not remain constant in each voxel as well. Adavi et al. (2022) proposed a method for the pre-analysis of the GNSS tomography solutions. They used the spread of the resolution matrix as an indicator to predict the accuracy of the tomography model. Since the method does not use any reference field (a priori information on the atmosphere) it cannot suggest appropriate resolutions for a tomographic model both in space and time. Sadeghi et al. (2022) proposed a method to determine the optimal resolution of a tomography model in space (horizontal size of voxels). The method takes the spatial changes of atmosphere into account using an initial reference model. As the result, they proposed a hybrid tomography model for their test area.

In this study we apply a method to determine a lower bound limit for the time resolution of tropospheric tomography which not only considers the adequacy of observations, but also incorporates the dynamics of water vapor in the study area. Our proposed method is based on the Empirical Orthogonal Functions (EOFs) constructed using the Weather Research and Forecasting (WRF) model as a priori information on the dynamics of atmosphere. The time resolution of our tomographic model is determined by using the EOFs in each layer of the model.. Moreover, we apply the reconstructed images for the validation of the proposed method.

A short theory on GNSS tomography and the estimation of EOFs are explained in the next section. Our method for the determination of time response follows the theoretical considerations. Then, we apply our approach to GPS measurements in two days, a day with high humidity and a day with low humidity. The section of numerical results reports the outcomes and discusses on the pros and cons of the proposed method. Concluding remarks are given in the last section.

Methodology

In this paper, the Empirical Orthogonal Functions (EOFs) method for constructing an optimal time response of a tomographic model has been applied. Therefore, a concise review on the GPS tomography is given first. Then,the EOFs and its application for estimating the optimal time response of a tomographic model is discussed.

GPS tomography, theory and method

The N_w which is mainly due to the water vapor, is a byproduct of the GNSS data processing algorithms. The reconstruction of the N_w is based on the formulation of the GPS signals wet delay in terms of the refractivity in the Earth's atmosphere. This gives a Fredholm Integral Equation (FIE) of the first kind as the mathematical model for this problem (Flores et al. 2000):

$$\mathbf{SWD} = 10^{-6} \int_s \boldsymbol{N}_w \, ds \tag{1}$$

Here, **SWD** stands for the Slant Wet Delay and s is the signal path between a satellite and a receiver. The continuous integral Eq. (1) is changed to a simultaneous system of linear equations by replacing the Earth's atmosphere using a 3D-mesh of cubes (known as voxels or the model elements) in which the refractivity is assumed to change only between such elements (Flores et al. 2000).

$$SWD_i = 10^{-6} \sum_{j=1}^{n} N_{wj} \, \Delta s_j \tag{2}$$

$$\mathbf{SWD} = \mathbf{A} \ \mathrm{N}_w \tag{3}$$

Here, j represents the j^{th} voxel and i is i^{th} GPS line of sight path with the length of Δs_j in this voxel (Rohm and Bosy 2009). Therefore, the lengths of the GPS signal segments in each voxel construct the rows of the design or coefficient matrix **A**. Then, GPS-tomography is a mixed determined inverse problem with a non-unique solution. To come up with a unique solution, the simultaneous system of observation equations is changed to a constrained system of equations.

A group of studies have focused on the application of different methods for constraining this problem: Some researchers used Meteorological observations (Hirahara 2000). Rohm and Bosy (2011) introduced additional parameters that obtained from the air flow analysis of radiosonde data and the COAMPS weather prediction model. Adavi and Mashhadi-Hossainali (2014) applied the observations of VRS to fix the rank deficiency of the problem.. We use the method of VRS in this study.The distribution of VRS

stations as well as the horizontal resolution of the model has been selected using the concept of model space resolution matrix (Adavi and Mashhadi-Hossainali 2014).

The total number of rows in **A** depends on the sampling rate of GNSS measurements and the time period in which our assumption on, the refractivity parameters is valid. This period of time is known as the time response of tomography. Selecting the appropriate value for this parameter is another challenge in GPS tomography: inappropriate time response results in the reconstructions that are not compatible with the dynamics of water vapor in the Earth's atmosphere. Moreover, small time responses not only increase the instability of the solution but also increase the number of the required constraints for computing a unique solution.

Since tomography is a large scale problem, recursive methods are normally used to acquire a regular solution (Elfving et al. 2010). We use the Landweber method, as a classic iterative regularization technique, for computing the solution. For the simultaneous equations $\mathbf{SWD} = \mathbf{A}N_w$ the Landweber solution is computed by (Elfving et al. 2010):

$$N_w^{s+1} = N_w^s + \lambda_s \mathbf{A}^T \left(\mathbf{SWD} - \mathbf{A}N_w^s\right) \tag{4}$$

where, is the relaxation parameter and is subjected to in order to guarantee the convergence of solution. Here, is the largest eigenvalue of **A** (Aster et al. 2018). We used the modified Ψ_2 strategy for computing relaxation parameter (Elfving et al. 2010).

Due to high accuracy, radiosonde is accepted as a reference for evaluating reconstructed images (Caldas-Alvarez et al. 2021, Adeyemi and Joerg 2012). Statistical quantities including Bias, Root Mean Square Error (RMSE) and Standard Deviation(Std) are the accepted and commonly used measures in this respect (Guerova 2003).

Empirical orthogonal functions

EOFs are analytic tools to understand the relationship of samples and variables. By determining the most important variabilities, EOFs help us link such variables to physical processes (Natali and Meza 2017).Basically, EOFs map an observation matrix (**X**) of p variables and n measurements onto a new orthogonal space. The new axes are toward the largest variances in the data (Fodor 2002). If **S** and **U** are score and loading matrix of **X,** respectively and r is the number of independent columns in **X** columns of **U** determine the directions of maximum variance in dataset. Then, **S** transforms original matrix to the new r-dimensional space. The dimension of the target space is reduced by constructing the transformation matrix **S** using the first k ($k \ll n$) EOFs. The key parameter k is determined through examining the input data (Fodor 2002).

EOFs are computed in either Q or R-modes. In the Q-mode, loading and score matrices are used to identify important samples and clusters of the variables. The R-mode is used in the classification of samples by discovering the relation of variable: The goal is identifying the important variables among the rest (Lee et al. 2017). Considering the aim of this study and the type of our data, R-mode has been applied for our analyzing in this research.

Datasets are classified into two major classes: non-spatial or typical versus spatial data. Non-spatial data incorporate the mere measurement of variables or their properties. Spatial data refer to data determined by a certain space or location attributed to the respective measurement (Demšar et al. 2013). SWDs are of spatial data kind. Therefore, we analyze EOFs using a certain analysis type which is suitable for spatial data.

Two analysis approaches can be applied on spatial data: The so-called standard method avoids spatial challenges altogether while in the second approach spatial effects such as spatial heterogeneity or autocorrelation are taken into account (Demšar et al. 2013). Based on our considerations for the selection of the R-mode, we prefer the standard analysis approach. This method is explained in the next section of this manuscript.

Non spatial analysis of spatial data

We use raster data analysis method for our investigations because it focuses on clustering, classification, change identification and tracking of specifications and properties. The method is only applied on spatial attribute(s). In other words, geographic effects are ignored. Moreover, an important assumption is that the cell sizes across the entire network are equal (Demšar et al. 2013).

Our Raster dataset is the data matrix in which the total number of columns and rows are equal to the number of measured variables and the number of cells in the network under study, respectively. Measured variables in each cell of every layer take up one column of the data matrix (seen Fig. 1).

Comparison of datasets

The comparison of the EOFs derived from multivariate samples helps discovering the similarities and differences of measured variables. For this comparison, we use the analytical method developed by (Krzanowski 1979).

Assuming multivariate samples **A** and **B** with transposed loading matrices **L** and **M**, respectively, which include p values of the same variables (x_1, ... , x_p) each measured n_1 and n_2 times, we have:

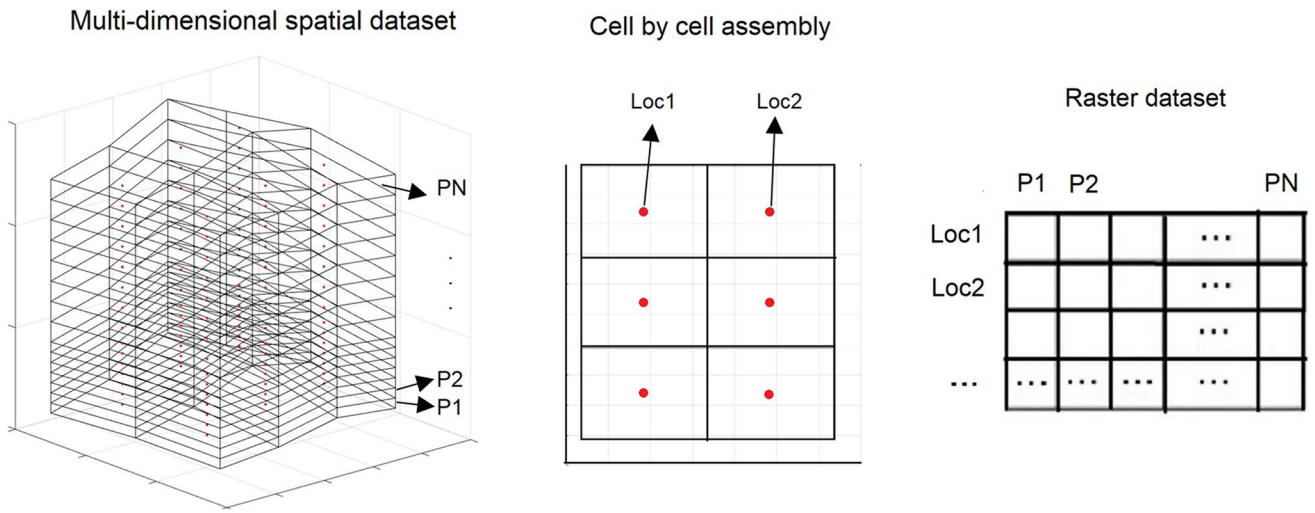

Fig. 1 Visualizing Raster dataset in space domain. Left: raster visualization of the research area. P1 … PN are the layers of the tomographic model in this research. Middle: location of the attributes assigned to each pixel. Voxels in a tomographic model are the pixels and Loc1, Loc2, etc. are the voxel centers in one of the layers in a tomographic model. Right: arrangement of Raster dataset

$$y_i = \sum_{j=1}^{p} l_{ij} x_j \quad , \qquad z_i = \sum_{j=1}^{p} m_{ij} x_j \qquad (i = 1, \ldots, k) \tag{5}$$

Here, y_i and z_i are the EOFs of datasets **A** and **B**, respectively. Dimensional reduction is done by keeping the first k EOFs, i.e. first k rows of matrices **L** and **M**. Transferred data are in the new k dimensional space with orthogonal axes $y_1, \ldots, y_k$ and $z_1, \ldots, z_k$.

Similarities and differences between datasets **A** and **B** is detected using eigenvalues of the matrix $\mathbf{F} = \mathbf{L}\mathbf{M}^T\mathbf{M}\mathbf{L}^T$ (Krzanowski 1979). If λ_1 is the largest eigenvalues of **F**, the coincidence angle $\left(\theta = \cos^{-1}\sqrt{\lambda_1}\right)$ between two subspaces of **A** and **B** can be used to find the value of k. The smallest angle is seen between a given vector of the first subspace and a vector from the second one which is almost parallel to it (resulting from its own map on the second subspace). Therefore, the sum of the eigenvalues of **F** equals the trace of **F** and equals the sum of the squares of the cosines between each of the k^{th} EOFs of two matrices **A** and **B**.

$$\sum_{i=1}^{k} \lambda_i = trace\ \mathbf{F} = \sum_{i=1}^{k}\sum_{j=1}^{k} \cos^2\theta_{ij} \tag{6}$$

This value is between k and zero. If the sum is equal to k, the two spaces are coincident and if zero, they are orthogonal. Therefore, this value can serve as a general criterion for the similarity of two datasets.

Numerical result and discussion

To investigate the proposed method, we consider two days with different weather conditions. Using the WRF model as our initial source of information on atmosphere, we analyze the EOFs for exploring the time variations of the N_w in our study area. To this end, this analysis is done for every height layer. The time intervals of this analysis are 30, 45, 60, 75, 90, 105 and 120 min, respectively. Using a previously designed tomographic model and taking these time intervals as the time response of this model, N_w images are reconstructed for each period, separately. Reconstructed images have been validated using radiosonde data. Based on the comparison of validation results, the optimum time response is suggested for our model. Finally, we compare this to the time period that our developed method suggests as the optimal time response for this model. This comparison is used to validate the efficiency of this method for selecting the time resolution in GNSS tropospheric tomography.

Study area and time

For our investigations to estimate optimal time resolution for a tomographic model using EOFs, GPS observations, Virtual Reference Station (VRS), radisonde profiles and weather parameters extracted from Weather Research

and Forecasting (WRF) model is required. Therefore, we selected an area of 24,000 km^2 located in the northwest of Iran as our experiment for various reasons including the widespread and relatively dense distribution of GPS stations as compared to other areas in Iran, its mountainous terrain being located in the foothills with diverse climates, and the reasonably accurate weather forecasting data availability.

The region includes15 GPS stations of the Iranian Permanent GPS Network (IPGN). Figure 2. shows the study region and the location of the applied GPS, VRS and radisonde stations for our evaluations.. The Bernese GPS software version 5.2 has been used for processing the GPS observations of the study days (i.e. DOYs 300 and 304).

The sounding data observed at UTC 00:00 at the Tabriz radiosonde station is used as a reference for evaluating reconstructed images in our study. Taking the relative humidity (derived from the radiosonde profiles) as the measure, we consider two distinct days: DOYs 300 and 304 of the year 2018 with high and low relative humidity, respectively. Figure 3 illustrates the vertical profile of relative humidity for both of the study days.

WRF model as a Numerical Weather Prediction (NWP) model predicts the 3D structure of the troposphere including temperature, specific humidity, pressure, height, etc. for 6, 12, 18,… to 120 h. In this study, we applied 24 h predictions on DOYs 300 and 304 of the year 2018. The spatial resolution of the applied WRF model is 10 km in space and 15-min in time.

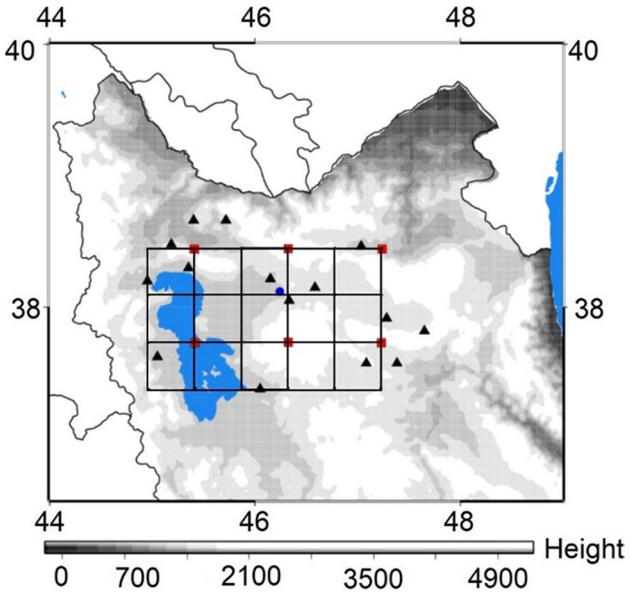

Fig. 2 Location of the investigated GPS stations (triangles),, VRS (squares) and the radiosonde station (circle) in the study area. The grid illustrates the top view of our tomographic model relative to the distribution of GPS stations

The reference NWP model and time responses

In GNSS tomography, the time resolution of the model is usually a constant parameter (for example, 1 h). In other words, tomographic images are reconstructed for or from every hour of GNSS measurements. However, wet

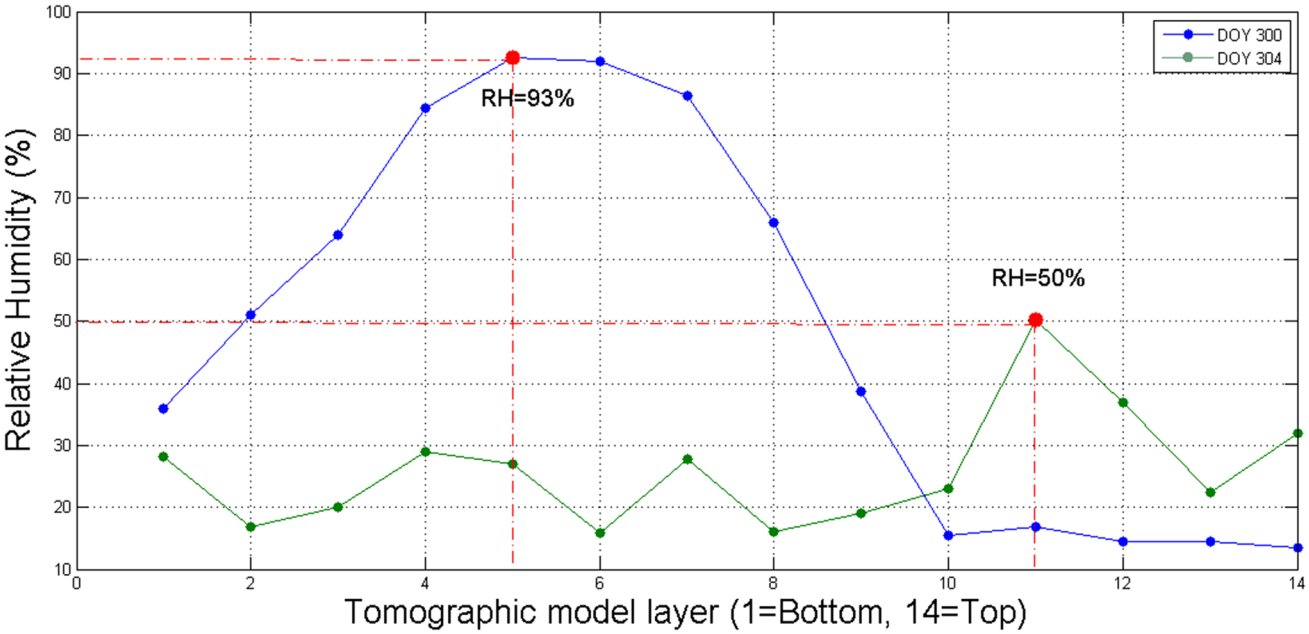

Fig. 3 Profiles of relative humidity (RH) from the first to the last layer of the tomographic model

refractivity (N_w) is a time dependent quantity. Therefore, in order to correctly capture the time variations of water vapor in reconstructed images, a chosen time resolution must conform to the ongoing variations of this parameter. In addition, an inappropriate chosen time response for the reconstruction of the N_w can increase the computational costs of the problem. This study proposes a method for the optimal selection of the time response in GNSS tomography. In this method pre-knowledge of the atmosphere is inevitable. Such information on the Earth's atmosphere is provided through the NWP models.

Assuming that the atmospheric condition can be stable during periods of 15 min, we consider this time interval as the reference time response. The horizontal resolution of our tomographic model is 40 km and the vertical resolution is 500 m to the height of 4 km and 1 km to an approximate height of 10 km from the surface of the ground. This spatial resolution together with the six VRS carefully selected for constraining the problem guarantees the uniqueness of our tomography solutions (refer to Fig. 2).

We apply time intervals of 30, 45, 60, 75, 90, 105 and 120 min for both days of our experiment as the time resolutions of our tomographic model. We compare the stability of atmospheric condition in each of these periods with the reference time response. The deesign matrices have been calculated for analyzing the rank deficiency of the problem using different time resolutions. In additional, resolution matrices have been calculated for investigating the percentage of the model parameters that are poorly resolved by the inverse solutions. These parameters are those whose resolution is either zero or close to zero (Aster et al. 2018). Tables 1 and 2 provide an overview on the relevant information.

According to Tables 1 and 2, increasing the temporal resolution of the tomographic model directly impacts the rank deficiency of the inverse solution. Lower time responses result in more poorly resolved parameters. Voxels with poorly resolved parameters are usually located in the lower layers or the layers that are near to the surface of the Earth. Moreover, increasing the time period of observations from 60 min in the wet and 45 min in the dry days of our experiment; do not reduce the rank deficiency of the problem. Based on this criterion only, the chosen time responses for our tomographic model could be 60 and 45 min in DOYs 300 & 304, respectively.

Table 1 Rank deficiency of coefficient matrix in DOY 300, 2018

Time-Response(min)	Number of observation	Rank deficiency	Poorly resolved (%)
30	9809	8	4
45	14,849	5	2.2
60	20,065	4	1.8
75	25,575	4	1.8
90	30,615	4	1.8
105	36,027	4	1.8
120	41,153	4	1.8

Table 2 Rank deficiency of coefficient matrix in DOY 304, 2018

Time-Response(min)	Number of observation	Rank deficiency	Poorly resolved (%)
30	9986	9	4
45	15,240	4	1.8
60	20,676	4	1.8
75	25,716	4	1.8
90	30,615	4	1.8
105	36,215	4	1.8
120	41,153	4	1.8

N_w scattering in height layers

To use EOFs for computing an appropriate time response for our tomographic model, the N_w values are computed at the position of the model grid points (Sadeghi et al. 2022). The atmospheric parameters for calculating N_w acquired from WRF model (Kleijer 2004).

We use the average of N_w values at the voxel grid points as the characteristic value in the corresponding voxel. Voxels in the same vertical layer are put together in one class as the measurements of one variable. This gives rise to a raster data set which is represented by a $(n \times p)$ matrix in which n is the number of measured units (the number of voxels in each layer of the model) and p is the number of vertical layers (variables). Since the horizontal resolution of our tomographic model is 40 km, it is easily seen that $n = 15$ and $p = 14$. Computed values of the first EOFs in both days and for the time spans of 30, 45, 60, 90, 105 and 120 min are illustrated in Fig. 4.

According to this figure, largest coefficients of the first EOFs are not seen in the same vertical layers: they are in the height layers 5 and 1 in DOYs 300 and 304, respectively. In other words, during the first day of our experiment, i.e. when the humidity was high, N_w has the highest scattering (in the measured units) in height layer 5 of our tomography model. This observation is confirmed by the vertical profile of RH as reported in Fig. 3. The next layers with highest scatter are height layers 4, 6 and 3, respectively.

In DOY 304, i.e. when the humidity is low, the largest coefficients of the first EOFs is observed in the first layer and therefore, the highest scattering of N_w happens in this layer. This observation is confirmed analogously by Fig. 3.

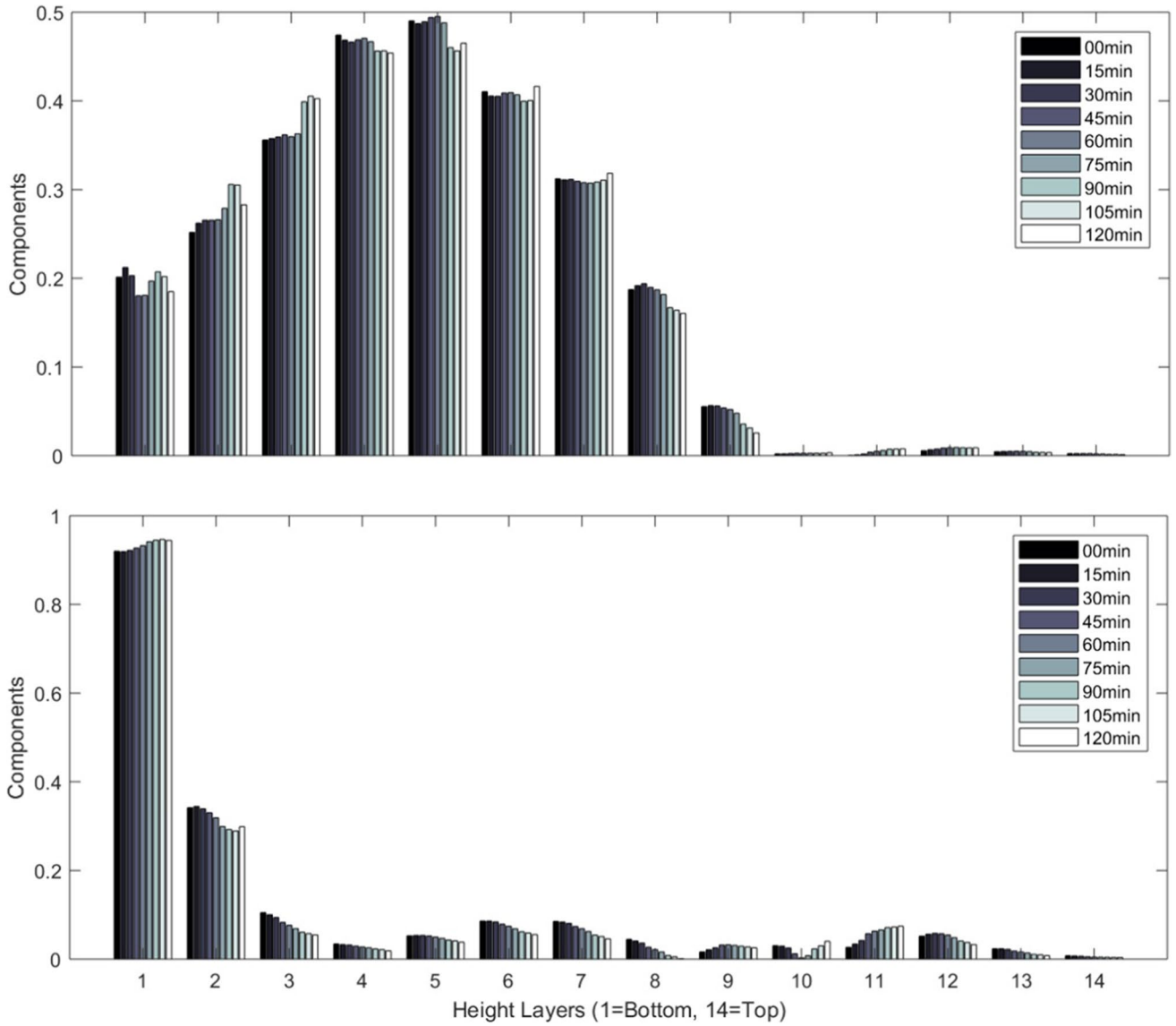

Fig. 4 First EOF of the constructed raster data for the tomography model of this study. Time responses of 15 to 120 min, in DOYs 300 (top) and 304 (bottom), 2018 are used

Estimating time response

By the application of an optimal time response, the reconstructed tomographic images are expected to include all information on the time variations of the N_w parameter. Obviously, smaller time responses provide more details on the time variation of the desired parameter. In GPS tomography, reducing the time interval of reconstructed images not only challenges the redundancy of the problem but also, increases its rank deficiency and therefore renders the accuracy of the solution. In order to infer an optimal time response for a tomography model, we propose to check the similarity of the model layers in the corresponding layers of a reference model. The time response of the reference model cannot be better than the temporal resolution of the NWP model.

We use EOFs for this comparison. The first challenge is finding a convenient dimension (k) for each subspace. This is usually done by trial and error: the ratio of the sum of k-largest to the total sum of eigenvalues ($\sum_{i=1}^{k}\lambda_i \Big/ \sum_{i=1}^{p}\lambda_i$) is usually used for this purpose (Deměsar et al. 2013). In this study, when $k=3$, subspaces retain 99% of the total variations in the original data. Therefor, 3-dimensional subspaces have been compared with one another.

Next, using the sum of the eigenvalues of **F** as a criterion to explore the similarity of two subspaces (if the sum is

3, then the two subspaces coincide or are identical, and if the sum is 0, the two subspaces are orthogonal) in the time domain, various time intervals are taken into account. In tropospheric tomography, the time response of tomographic model usually is in the range of 30 to 120 min. In near real-time applications, the time response is 15 min. Therefore, we performed this analysis using the time resolutions of 15, 30, 45, 60, 75, 90, 105 and 120 min. The sum of the three largest eigenvalues of **F** for both days of this study is given in Table 3.

According to Table 3, the dissimilarity of scattering in the N_w parameter between the WRF model and its subspace of 15 min is almost zero. Nevertheless, it is not feasible to use this time interval as the time response for GPS-tomography in our test area. Because, many of the diagonal elements in the resolution matrix become either zero or close to zero. In other words, N_w will be poorly resolved in a wide area. On the other hand, according to Tables 1 and 2 the area with poorly resolved unknowns is minimized if the time response is 60 and 45 min in the wet and dry days of our experiment. Based on Table 3, this would be at the cost of 6% and 3% dissimilarity between the dynamics of the N_w in reconstructed images and the WRF model.

The above outcomes are valid if the accuracy of the applied numerical weather model is at least 94% and 97%, in the study days of this research. To analyze the accuracy of our WRF model, we compared this model with our radiosonde profile. Table 4 reports on the relevant results.

Based on radiosonde data and on average; the similarity of the N_w derived from the WRF model and radiosonde data is not better than 85% in DOY 300. This increases to 93% in the dry day of our experiment. Furthermore, Table 3 implies that the minimum time response that we can propose for our tomographic model is between 75 to 90 min in DOY 300 and about 60 to 75 min in DOY 304.

Table 3 Sum of the eigenvalues of **F** in 3D subspaces and the percentage of similarity of subspaces with the reference model

Temporal Resolution	DOY 300		DOY 304	
	$\sum_{i=1}^{3} \lambda_i$	Coincident percentage	$\sum_{i=1}^{3} \lambda_i$	Coincident percentage
0–15 min	2.97	99	2.99	≈100
0–30 min	2.92	97	2.95	98
0–45 min	2.87	96	2.91	97
0–60 min	2.81	94	2.83	95
0–75 min	2.65	88	2.80	94
0–90 min	2.49	83	2.78	93
0–105 min	1.99	66	2.77	92
0–120 min	2.34	78	2.78	93

Validation of proposed time responses

The bias and Std of the reconstructed N_w fields are expected to be the first minimal values for the proposed time responses when the regularization parameter and the initial field used for finding the inverse solutions are the same. Based on this idea we have reconstructed the N_w field using our radiosonde data as the a-priori information that we need for finding the inverse solutions.

Reconstructing N_w filed

To compare the impact of different time responses on reconstructed images, N_w has been also reconstructed using the time intervals of 30, 45, 60, 75, 90, 105 and120 minutes in our study area and for DOYs 300 and 304. The spatial resolution of the model is as before. Reconstructed images have been validated using the N_w profiles that we derived from radiosonde data. Figure 5 demonstrates the reconstructed and validation profiles. The statistical quantities of Bias, RMSE, and Std have been used to validate the reconstructed images. Corresponding results are given in Table 5.

Table 5 also shows that the quality of the reconstructed model parameters depends on the time resolution of the model. Moreover, since the validation is done in a certain column of our model, the reported parameters (i.e. the bias and standard deviation) are representatives for the quality of reconstructed images in this part of the model.

Based on previous discussion, in DOY 300; the maximum overall similarity of the reference and tomographic models is about 85%. This similarity is expected when the time

Table 4 Statistics for the WRF N_w profile as compared to the radiosonde profile

DOY	Statistical measures	Time Resolution (min)						
		30	45	60	75	90	105	120
300	Bias	-3.81	-3.69	-3.48	-3.2	-3.03	-3.52	-3.10
	RMSE	5.08	5.04	5.02	4.70	4.22	4.86	4.60
	Std	3.36	3.44	3.61	3.40	2.94	3.35	3.39
304	Bias	0.55	0.33	0.59	0.14	0.32	0.27	0.08
	RMSE	1.38	1.22	1.62	0.93	0.83	1.24	0.93
	Std	1.27	1.17	1.51	0.92	0.77	1.21	0.93

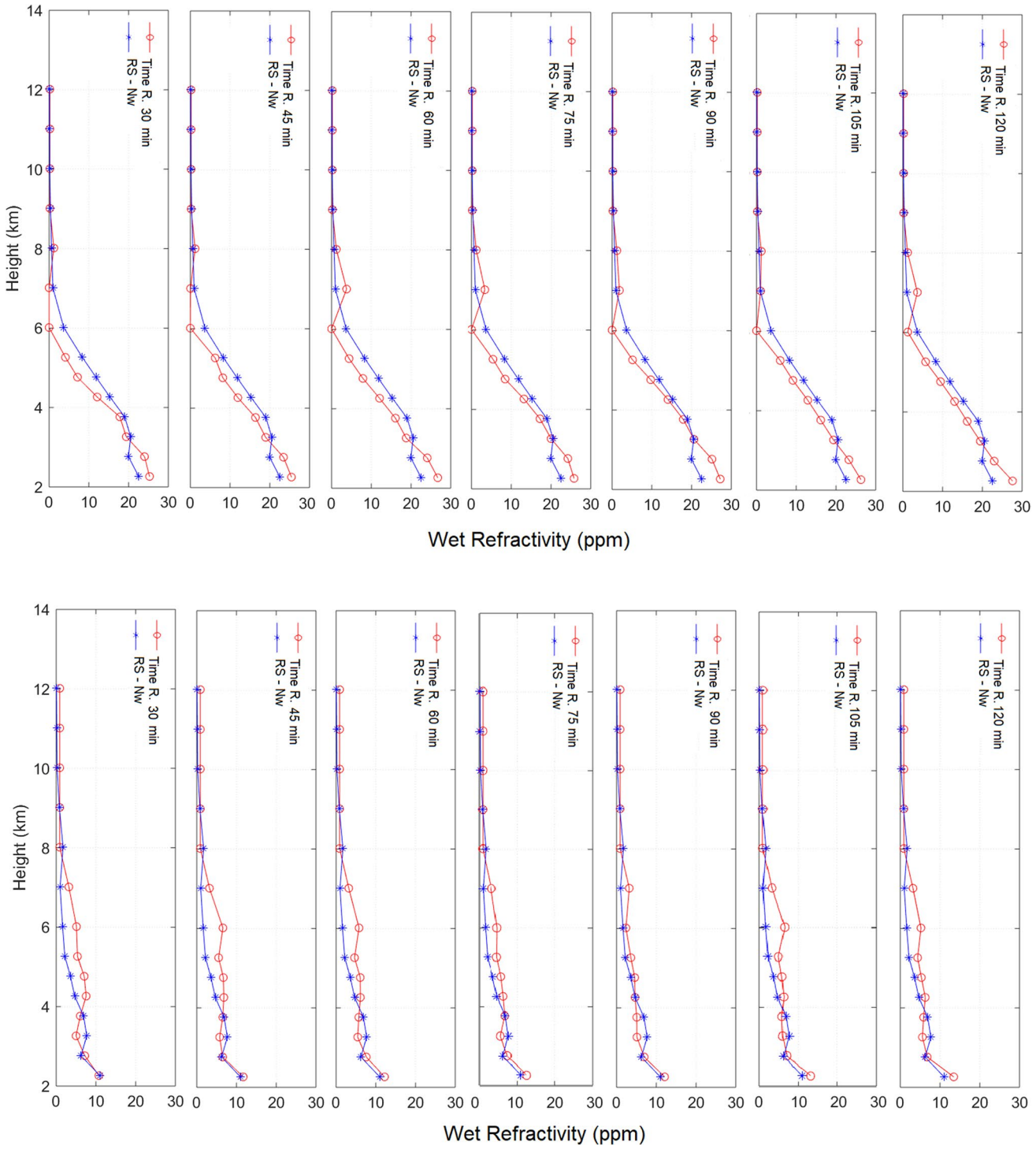

Fig. 5 N_w profiles reconstructed by tomographic model and derived from radiosonde data (non-solid versus stars) for the time intervals: 30, 45, 60, 75, 90, 105 and 120 min of DOYs 300 (top) and 304 (bottom), 2018

resolution of the model is between 75 and 90 min. According to Table 5, in DOY 300; the bias and standard deviations are almost equal when the time resolution of the model is 75, 90 or even 105 min. Moreover, the very first inverse solutions with minimal bias and minimal Std are obtained for the time responses of 75 and 90 min in the wet day of this study. Furthermore, Table 5 shows that the very first inverse solutions with minimal bias and minimal Std are obtained for the time responses of 60 to 75 min in the dry day of this study. This confirms that the proposed method can provide

Table 5 Bias, RMSE and Std of reconstructed images with respect to the radiosonde N_w profiles

DOY	Statistical measure	Time Resolution (min)						
		30	45	60	75	90	105	120
300	Bias	-0.83	-0.77	-0.56	-0.27	0.02	-0.52	-0.15
	RMSE	2.55	2.29	2.79	2.33	2.4	2.18	2.31
	Std	2.41	2.15	2.74	2.32	2.4	2.12	2.31
304	Bias	0.99	1.14	0.59	0.97	0.3	1.1	0.9
	RMSE	2.05	2.09	1.74	1.66	1.26	2.00	1.74
	Std	1.79	1.76	1.64	1.34	1.23	1.68	1.48

initial information on the minimum required time period as the time response of our tomographic model.

Conclusion

This study introduces a method for determining the time response of a tomographic model. Proposed method is based on the analysis of EOFs. The method is used for reconstructing the N_w in Northwest of Iran. This study area was selected to test the efficiency of this method due to mountainous terrainand the relatively dense GPS network. Virtual reference stations have been used for computing a unique solution to the problem. Two days with different relative humidity have been studied for analyzing the efficiency of the proposed method i.e. DOY 300 and 304 of 2018 with high and low relative humidity, respectively. The WRF model with spatiotemporal resolutions of 10 km and 15 min were used as the initial information on the atmosphere in our test area. The time resolutions: 30, 45, 60, 75, 90, 105 and 120 min have been taken as the time response of a previously deigned tomographic model in this area. Based on the analysis of EOFs, using the time responses of 60 to75 and 75 to 90 min; the similarity of the scattering between the reconstructed images and the reference model are expected to be 85% and 93% for the wet and dry days in our experiments. Since proposed time responses are computed only using a reference field, our method can be used as a pre-analysis tool for not only determining the time resolution in GPS tropospheric tomography, but also provides information on the atmospheric dynamics that could be expected in reconstructed images.

Acknowledgements We are grateful of National Cartographic Center (NCC) of Iran, for providing the observation files of the northwest part of the Iranian Permanent GPS Network (IPGN). We particularly appreciate Iran meteorological organization for access to radiosonde profiles with dense pressure levels at the evaluated station in this research. We are grateful to Mrs. Mohamadi, researcher in Atmospheric Science and Meteorological Research center of Iran for providing the NetCDF files extracted from the WRF model.

Author Contribution ES and MMH designed the research and wrote the main manuscript text. AS provided the observation files of the northwest part of the Iranian Permanent GPS Network (IPGN). ES did formal analysis and investigations. ES and MMH interpreted the output results. MMH investigated and approved the results. All authors reviewed and approved the final version of manuscript.

Data availability All the datasets used in this study can be obtained from the corresponding author.

Declarations

Competing interests The authors declare no competing interests.

Conflict of interest The authors declare that they have no conflicts of interest.

References

Adavi Z, Mashhadi-Hossainali M (2014) 4D tomographic reconstruction of the tropospheric wet refractivity using the concept of virtual reference station, case study: northwest of Iran. Meteorol Atmos Phys 126(3):193–205

Adavi Z, Weber R, Rohm W (2022) Pre-analysis of GNSS tomography solution using the concept of spread of model resolution matrix. J Geodesy 96(4):1–12

Adeyemi B, Joerg S (2012) Analysis of water vapor over Nigeria using radiosonde and satellite data. J Appl Meteorol Climatol 51(10):1855–1866

Aster RC, Borchers B, Thurber CH (2018) Parameter estimation and inverse problems. Elsevier

Bender M, Dick G, Ge M, Deng Z, Wickert J, Kahle H-G, Raabe A, Tetzlaff G (2011) Development of a GNSS water vapour tomography system using algebraic reconstruction techniques. Adv Space Res 47(10):1704–1720

Bender M, Dick G, Heise S, Zus F, Deng Z, Shangguan M, Ramatschi M, Wickert J (2013) GNSS water vapor tomography. In Deutsches Geo Forschungs Zentrum. GFZ

Bender M, Dick G, Wickert J, Ramatschi M, Ge M, Gendt G, Rothacher M, Raabe A, Tetzlaff G (2009) Estimates of the information provided by GPS slant data observed in Germany regarding tomographic applications. J Geophys Res Atmos 114(D6)

Bevis M, Businger S, Herring TA, Rocken C, Anthes RA, Ware RH (1992) GPS meteorology: Remote sensing of atmospheric water vapour using the global positioning system. J Geophys Res Atmos 97(D14):15787–15801

Caldas-Alvarez A, Khodayar S, Knippertz P (2021) The impact of GPS and high-resolution radiosonde nudging on the simulation of heavy precipitation during HyMeX IOP6. Weather and Climate Dynamics 2(3):561–580

Deňsar U, Harris P, Brunsdon C, Fotheringham AS, McLoone S (2013) Principal component analysis on spatial data: an overview. Ann Assoc Am Geogr 103(1):106–128

Dong Z, Jin S (2018) 3-D water vapor tomography in Wuhan from GPS, BDS and GLONASS observations. Remote Sens 10(1):62

Elfving T, Nikazad T, Hansen PC (2010) Semi-convergence and relaxation parameters for a class of SIRT algorithms. Electron Trans Numer Anal 37(274):321–336

Flores A, Ruffini G, Rius A (2000) 4D tropospheric tomography using GPS slant wet delays. In Annales Geophysicae, 18:223–234. Springer

Fodor IK (2002) A survey of dimension reduction techniques. (No. UCRL-ID-148494). Lawrence Livermore National Lab., CA (US)

Guerova G (2003) Application of GPS derived water vapour for numerical weather prediction in Switzerland. Doctoral dissertation University of Bern

Haji-Aghajany S, Amerian Y, Verhagen S, Rohm W, Ma H (2020a) An optimal troposphere tomography technique using the WRF model outputs and topography of the area. Remote Sens 12(9):1442. https://doi.org/10.3390/rs12091442

Haji-Aghajany S, Amerian Y, Verhagen S (2020b) B-spline function-based approach for GPS tropospheric tomography. GPS Solutions 24(3):1–12

Heublein M, Alshawaf F, Erdnüß B, Zhu XX, Hinz S (2019) Compressive sensing reconstruction of 3D wet refractivity based on GNSS and InSAR observations. J Geod 93:197–217

Hirahara K (2000) Local GPS tropospheric tomography. Earth Planet Sp 52(11):935–939. https://doi.org/10.1007/s00190-018-1152-0

Kleijer F (2004) Troposphere modeling and filtering for precise GPS leveling, Delft Univ. of Technol., Delft, Netherlands

Krzanowski W (1979) Between-groups comparison of principal components. J Am Stat Assoc 74(367):703–707

Lee LC, Liong C-Y, Jemain AA (2017) Q-mode versus r-mode principal component analysis for linear discriminant analysis (LDA). In AIP Conference Proceedings, volume 1842, page 030024. AIP Publishing LLC

Natali MP, Meza A (2017) PCA and vTEC climatology at midnight over mid-latitude regions. Earth Planets Space 69(1):1–22

Rohm W, Bosy J (2009) Local tomography troposphere model over mountains area. Atmos Res 93(4):777–783

Rohm W, Bosy J (2011) The verification of GNSS tropospheric tomography model in a mountainous area. Adv Space Res 47:1721–1730. https://doi.org/10.1016/j.asr.2010.04.017

Sadeghi E, Mashhadi Hossainali M, Safari A (2022) Development of a hybrid tomography model based on principal component analysis of the atmospheric dynamics and GPS tracking data. GPS Solutions 26(3):1–13

Trzcina E, Rohm W (2019) Estimation of 3D wet refractivity by tomography, combining GNSS and NWP data: first results from assimilation of wet refractivity into NWP. Q J R Meteorol Soc 145:1034–1051. https://doi.org/10.1002/qj.3475

Wang X, Dessler AE (2020) The response of stratospheric water vapor to climate change driven by different forcing agents. Atmos Chem Phys 20(21):13267–13282

Yao Y, Zhao Q (2016) Maximally using GPS observation for water vapor tomography. IEEE Trans Geosci Remote Sens 54(12):7185–7196